

Numerical permeability tensor characterization of fibrous reinforcement through 1D flow analysis using particle swarm optimization

Salman Zafar^{1,2,3}, Hatice S. Sas^{*1,2,3}

¹Integrated Manufacturing Technologies Research and Application Center. Sabanci University. Orhanli- Tuzla. 34956 ISTANBUL, TURKEY

² Faculty of Engineering and Natural Sciences. Sabanci University. Orhanli-Tuzla. 34956. ISTANBUL, TURKEY

³Composite Technologies Center of Excellence. Sabanci University-Kordsa. Istanbul Technology Development Zone. Pendik. 34906 ISTANBUL, TURKEY

(Alınış / Received: 10.08.2022, Kabul / Accepted: 29.11.2022, Online Yayınlanma / Published Online: 30.12.2022)

Keywords

Fibrous reinforcement,
Permeability tensor,
Flow Simulations,
Particle Swarm
Optimization

Abstract: Flow simulations are performed to analyze the resin flow behavior through fibrous reinforcements to promote void-free composite manufacturing with excellent mechanical properties. These flow simulations require an essential parameter known as permeability tensor which is defined as the resistance to the flow of resin due to fibrous reinforcement. This study proposes a key strategy to determine all in-plane permeability components from a single rectilinear flow experiment. The proposed method is based on introducing intentional disturbance to the mold domain, which transforms the one-dimensional flow into a two-dimensional flow. The process is divided into two steps, the experimental determination of flow arrival times at designated locations within the mold domain and comparing it to the numerical flow arrival times (obtained using LIMS software) via the residual sum of squares (RSS). An optimization algorithm based on particle swarm optimization (PSO) is established to reduce the RSS to get accurate permeability predictions. The validation study of the proposed strategy has been practiced for three cases. The results show that this method can effectively characterize the in-plane permeability components from a single rectilinear injection experiment.

Parçacık sürüsü optimizasyonu ile 1-boyutlu akış analizi yoluyla kompozit kumaşların geçirgenlik tensörünün sayısal karakterizasyonu

Anahtar Kelimeler

Lifli takviye,
Geçirgenlik tensörü,
Akış Simülasyonları,
Parçacık Sürü
Optimizasyonu

Öz: Akış simülasyonları, yüksek mekanik özelliklere sahip boşluksuz kompozit üretimini teşvik etmek için lifli takviyeler yoluyla reçine akış davranışını analiz etmek için gerçekleştirilir. Bu akış simülasyonları, lifli takviye nedeniyle reçine akışına karşı direnç olarak tanımlanan, geçirgenlik tensörü olarak bilinen önemli bir parametre gerektirir. Bu çalışma, tek doğrusal enjeksiyondan tüm düzlem içi geçirgenlik bileşenlerini belirlemek için anahtar bir strateji sunmaktadır. Yöntem, bir-boyutlu akışı iki-boyutlu bir akışa dönüştüren, kalıp alanına kasıtlı bir düzensizlik bölgesinin tanımlanmasına dayanmaktadır. Öncelikle, kalıp alanı içinde belirlenmiş konumlardaki akış varış zamanlarının deneysel olarak belirlenmesi ve bunu, artık kareler toplamı (RSS) yoluyla LIMS yazılımı ile elde edilmiş sayısal akış varış zamanlarıyla karşılaştırılmaktadır. Geçirgenlik tahminlerini hızlı ve yüksek doğrulukta elde etmek için parçacık sürüsü optimizasyonuna (PSO) dayalı bir optimizasyon algoritması kurulmuştur. Önerilen stratejinin validasyon çalışması üç farklı geçirgenlik tensörü durmunu ile yapılmıştır. Sonuçlar, bu yöntemin, tek bir doğrusal enjeksiyon deneyi ile düzlem içi geçirgenlik bileşenlerini etkili bir şekilde karakterize edebildiğini göstermektedir.

*Corresponding Author, email: hatice.sas@sabanciuniv.edu

1. Introduction

Liquid composite molding (LCM) is a composite manufacturing process widely adapted across numerous industries. In this process, a dry fibrous reinforcement in the shape of the final part geometry is placed in a mold, and then a liquid resin system is allowed to flow through the reinforcement under the action of applied pressure difference. The liquid resin is then allowed to cure, after which the composite is demolded. The resin must fill all the empty spaces within the fibrous reinforcement so that the resulting composite is void-free and has excellent mechanical properties. To achieve this, it is essential to analyze and control the flow of resin through the reinforcement. An effective way to analyze the resin flow is to model it numerically. Mathematically, the flow of resin through the fibrous reinforcement can be modeled as flow through porous media by using Darcy's law:

$$\langle \mathbf{u} \rangle = -\frac{\mathbf{K}}{\mu} \cdot \nabla p \quad (1)$$

where $\langle \mathbf{u} \rangle$ is the volume-averaged flow velocity, μ is the resin viscosity, ∇p is the applied pressure gradient across the gate and vent locations, and \mathbf{K} is the permeability tensor. Permeability is defined as the resistance to flow of the resin due to the fibrous reinforcement. It is an essential input parameter for resin flow simulations to design and optimize gate and vent locations and other manufacturing parameters for LCM processes [1–3]. Permeability tensor is represented as a second-order symmetric tensor, and for fluid flow in an anisotropic media, it is given as:

$$\mathbf{K} = \begin{bmatrix} K_{xx} & K_{xy} & K_{xz} \\ K_{xy} & K_{yy} & K_{yz} \\ K_{xz} & K_{yz} & K_{zz} \end{bmatrix} \quad (2)$$

In composite processing design, the accuracy of the permeability tensor plays such a crucial role that there have been many attempts to characterize it. All the characterization methods presented in the literature [4]–[10] can be divided into two main categories based on their injection methods: radial injection and rectilinear injection flow. Radial injection allows the determination of complete in-plane permeability tensor from a single experiment, whereas rectilinear injection requires at least three experiments. This fundamental difference between radial and rectilinear injection methods makes the former method more attractive because of the fewer experimental efforts. However, it has been established that results obtained from radial injection have high variations and are not reproducible [10]–[12]. On the other hand, the reproducibility of permeability results via rectilinear injection has been confirmed in an international benchmark study [13].

There have also been many attempts to determine dual scale or three-dimensional (3D) permeability using numerical methods [14]. In 3D permeability, through-thickness resin flow behavior is also considered along with the planar flow; hence, Eq (2) can represent three additional permeability components, i.e., K_{zz} , K_{xz} , and K_{yz} . Okonkwo et al. [15] used the radial flow method and optimization routine to characterize 3D permeability, while Yun et al. [16] explored a similar approach to characterize the 3D permeability for thick preforms. Gokce et al. [17] used the rectilinear injection method to characterize the transverse permeability with the help of preform with previously known in-plane permeability components.

Despite its ability to provide accurate permeability predictions, not much work has been done to reduce the experimental efforts involved in the rectilinear injection method; therefore, the focus of this study is to utilize this technique for in-plane permeability characterization and to reduce the related complexities. Lundström et al. [4] proposed a multi-cavity rectilinear flow technique to determine in-plane permeability tensor from a single experiment. Di Fratta et al. [5] suggested a strategy to use flow front angle for complete determination of in-plane permeability tensor using two rectilinear flow measurements. Moreover, Lugo et al. [18] developed an analytical method to determine in-plane permeability (in flow direction) as well as the permeability in the through-thickness direction from a single rectilinear experiment. The method depends on the use of preform partially covered with distribution media (a highly permeable layer). The presence of distribution media introduces a flow difference between the top and bottom of the preform, causing two-dimensional (2D) flow conditions in the through-thickness direction. This phenomenon provides the means to estimate the through-thickness permeability from the same single experiment. The aforementioned studies have shown that it is possible to determine textile permeability with fewer experiments than required when using the rectilinear injection method. However, the number of the experiments needed to determine in-plane permeability via the rectilinear method can be further reduced, and the process can be simplified.

This study presents a new and improved methodology to characterize all three components of the in-plane permeability tensor (K_{xx} , K_{xy} , and K_{yy}) from a single rectilinear flow experiment. The main idea of the proposed method is to determine all three components of the in-plane permeability tensor by utilizing the intentionally introduced disturbance to the unidirectional (1D) resin flow in the in-plane space. The resin arrival times at

different sensor locations are recorded during the resin flow. Then, an optimization routine is created using the particle swarm optimization (PSO) method in which the permeability values in a flow simulation of a similar domain are updated continuously until the error between arrival times from simulation and experiment is minimized.

2. Methodology

2.1. In-plane Permeability Tensor Characterization

The objective of this study to use a single rectilinear experiment to characterize in-plane permeability components is based on the introduction of disturbance to the mold domain. The numerical simulation for the flow through porous media is performed with Liquid Injection Molding Simulation (LIMS). LIMS [19] is a finite element/control volume-based method that uses Darcy's law to simulate the mold filling process of resin transfer molding (RTM) and other related processes. LIMS can be used to optimize gates and vent locations in a mold and design injection scheme which allows to strategically control the resin flow into the mold [20,21]. However, LIMS needs permeability tensor values, resin viscosity, fiber volume fraction, and boundary conditions to simulate the resin flow and gives resin arrival time for each node of discretized geometry.

The mold domain used in this study is shown in Figure 1 along with its dimensions and the corresponding mesh. The dimensions of mold in both cases are 0.5 m x 0.2 m, while the dimensions of the rectangular disturbance located at the top-left of the mold domain are 0.1 m x 0.04 m. The dimension and position of the rectangular disturbance will not have any effect on the prediction behavior. A transversely anisotropic preform of 0.5 fiber volume fraction (with $K_{xx} = K_{yy} = 5.65 \times 10^{-10} \text{ m}^2$ and $K_{xy} = 0$) and rectilinear linear injection is considered along the x-direction for both cases. Moreover, the left side of the mold is assigned as inlet gate with $1 \times 10^5 \text{ Pa}$ pressure, whereas the right side is considered to be the vent for the flow of the resin having a viscosity of 0.1 Pa.s. Figure 2 and Figure 3 present the fill time behavior and pressure distribution, respectively, for both cases i.e., for a regular mold and a mold with the rectangular disturbance. Figures 2(b) and 3(b) demonstrate the changes in fill-time behavior and pressure distribution experienced by the flowing resin due to the presence of the rectangular disturbance in the mold. As shown in Figure 2(b), the disturbance in the mold affects the fill time behavior and results in two velocity components, i.e., in x- and y-direction. Similarly, the pressure distribution in Figure 3(b) shows two components of pressure gradient, indicating that the initial 1D flow transformed into a 2D flow. This transformation of the flow is extremely crucial in determining all in-plane permeability components from a single rectilinear experiment. Also, the proposed methodology is highly dependent on the resin fill time.

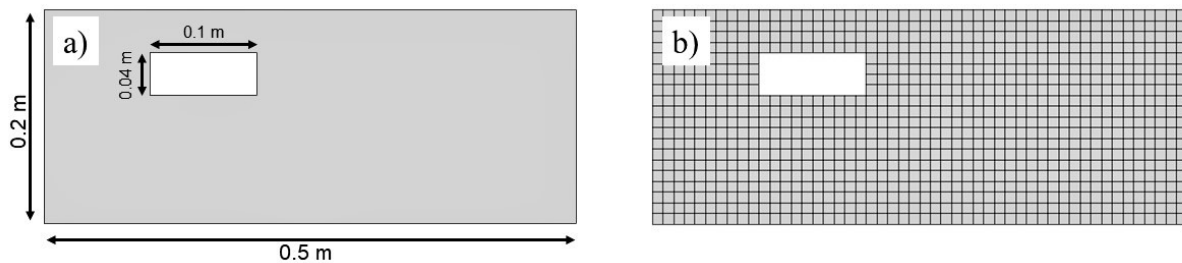


Figure 1. (a) Dimensions and (b) Mesh of the mold domain used in this study.

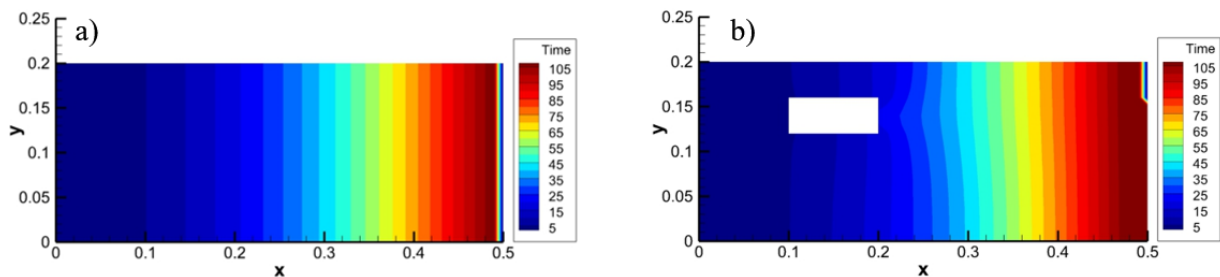


Figure 2. Fill time (seconds) behavior for transversely anisotropic preform in (a) regular mold and (b) mold with rectangular disturbance.

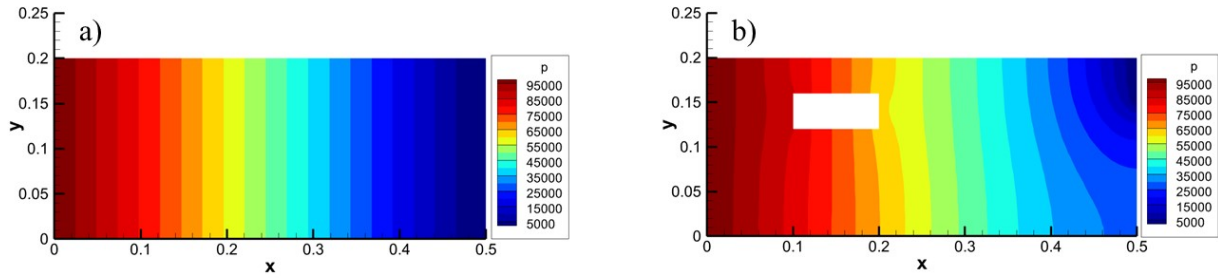


Figure 3. Pressure (Pa) distribution for transversely anisotropic preform in (a) regular mold and (b) mold with rectangular disturbance.

The steps involved in this study to characterize the permeability components are summarized in Figure 4. The first step is to conduct the virtual 1D flow experiment to record the experimental flow arrival time ($T_{i,exp}$) for the assigned in-plane permeability tensor. In the second step, LIMS is used to compute numerical resin arrival time ($T_{i,LIMS}$) for the permeability tensor values of the upper and lower limits of the search domain. The flow arrival time obtained from LIMS is then compared to experimentally recorded resin arrival time and manipulated continuously by updating the permeability tensor guess to reduce the residual sum of squares (RSS). The RSS between the experimental and simulated flow arrival time is used as a parameter to quantify their difference. RSS is calculated as follows:

$$RSS = \sum_{i=1}^N (T_{i,exp} - T_{i,LIMS})^2 \quad (3)$$

In Eq (3), N is the total number of nodes in a discretized geometry and/or corresponding sensors to detect the position of resin in an experimental setup, $T_{i,exp}$ is virtual experimental flow arrival time and $T_{i,LIMS}$ is simulated flow arrival time at i^{th} node/sensor.

The accuracy of the predicted results depends on the minimization of RSS, and for this purpose different optimization algorithms can be used. Okonkwo et al. [15] used the Golden Section Search Minimization Technique (G2MST), and Yun et al. [16] used Simplex Algorithm to characterize 3D fabric permeability. However, in both cases, determination of the initial permeability values was the initial requirement to execute the optimization process. Therefore, in this study, a population-based stochastic technique named Particle Swarm Optimization (PSO) is used to minimize RSS, which does not require initial guesses to start the optimization process.

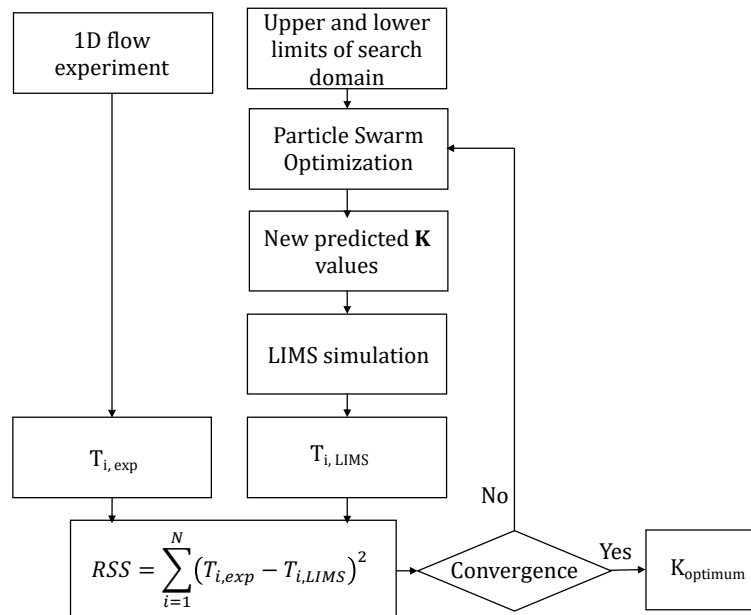


Figure 4. Methodology for the characterization of all in-plane permeability components via single rectilinear injection experiment.

2.2. Particle Swarm Optimization

Particle Swarm Optimization (PSO) is a population-based optimization method initially developed by Eberhart et al. [22]. The inspiration behind the development of PSO was derived from the socializing behavior of bird flocking and fish schooling. A key advantage of using the PSO algorithm is that it requires low computational cost. PSO applies social laws to search for the global optimum in a design space. The optimization process of PSO starts by introducing a population of particles randomly distributed at various locations in a search domain, where the location of each particle represents a specific solution. Due to the random distribution of particles, each particle is at a different location in a search domain, and to achieve an optimum, the particles need to update their positions continuously. The change in a particle's position changes its corresponding velocity, resulting in a continuous velocity update. The velocity update that corresponds to the best position of the particle is the key operator behind the optimization process of the PSO algorithm. The best position/location is defined as the nearest position to the possible optimum solution. In PSO, the overall best position is evaluated by considering the best of all particles (global best position) and the best of an individual particle (local best position) that it has reached during the search. This critical approach of PSO helps the entire population of particles to migrate toward the global optimum. Each particle's velocity and position are updated stochastically at each iteration during the optimization process using the following relationships.

$$V_i^{t+1} = \omega V_i^t + C_1 r_1^t (P_i^t - X_i^t) + C_2 r_2^t (P_g^t - X_i^t) \quad (4)$$

$$X_i^{t+1} = X_i^t + V_i^{t+1} \quad (5)$$

In Eq (4) and Eq (5), V_i^t and X_i^t are velocity vector and position vector, respectively. P_i^t refers to the best position of an individual particle, while P_g^t represents the global best position of the whole population. Eq (4) explains the velocity update criteria of the PSO algorithm. It contains three terms, the first of which represents inertia, the second term refers to cognitive behavior, and the third term represents the social behavior of particles. Each term has its respective coefficients ω , C_1 , and C_2 which control the exploration and exploitation behavior of the particles. ω , known as inertia coefficient, defines the ability of the population to change its direction and, as the name suggests, represents the inertia of the population. Higher values of ω encourage exploitation whereas lower values facilitate exploration. Thus, a suitable value of ω can provide a balance between exploration and exploitation. C_1 influences the individualistic behavior of the population; therefore, higher C_1 makes it very difficult to achieve convergence as each particle tries to focus on its best solution. On the other hand, C_2 enforces the influence of particles on each other and improves the collective behavior of the population.

3. Results and Discussion

The accuracy of the presented methodology is evaluated by considering a filling of 0.5 m x 0.2 m x 0.005 m rectangular mold with a constant inlet pressure of 1×10^5 Pa (Figure 1). The fiber volume fraction is 0.5, while the resin viscosity is 0.1 Pa.s. It is very challenging to control the variations in the predicted permeability values during actual experiments. In this study, to validate the presented methodology for permeability characterization, virtual experimentations are performed. In a virtual experiment, a simulation is performed via LIMS by providing permeability values (considered as 'ground value'). This virtual experiment provides flow arrival time ($T_{i,exp}$) at each node of discretized geometry (Figure 1(b)). The position of these nodes corresponds to the position of sensors in an actual experiment. The methodology presented in the previous section is then used to predict the permeability components, which are then compared with ground permeability values. To assess the efficiency of the methodology, three different cases were tried: (i) predicting permeability components in flow direction by using regular mold domain with isotropic preform only, (ii) predicting all three anisotropic permeability components from a single injection by introducing the disturbance to mold domain, and (iii) predicting all three anisotropic permeability components from a single injection by introducing the disturbance to mold domain in the presence of race tracking phenomena as it is the main drawback of rectilinear injection [23], [24]. For each case, two different trials were executed and for each trial the same search domain size was used (upper and lower limits for search domain), while the population of particles was taken to be 200. The results are listed in Table 1. As described earlier as an advantage of using PSO, no initial guess values were needed to proceed with the prediction process. Thus, it can be concluded from the results presented in Table 1 that the proposed methodology is able to predict the permeability values in a very accurate manner. In almost all cases, the error between the ground value and the predicted value is less than 0.01%, with an exception in the second trial of case (ii), in which the maximum error obtained is 3.96%.

To further elaborate the role of PSO in permeability prediction in this study, an analysis on the evolution of particles' population has been performed. Since PSO relies on the convergence of the population to a single global solution, the statistical range of particles in each variable direction is plotted against the iteration to observe the population's behavior. The statistical range represents the spread of particles from each other. If the particle swarm converges to a single solution, then the range in each variable direction goes to zero. Otherwise, in some variable directions, it remains away from zero. The results obtained for case 2(a) of Table 1 are presented in Figure 5. It can be observed that since the beginning of the optimization process, the range is very small, implying that particles are already close to each other. The reason for this can be the upper and lower limits of the search domain used in this study.

The pressure distribution obtained for all three cases are presented in Figure 6. For the first case in Figure 5(a), the pressure gradient is parallel as no anisotropy is assumed. While for the second and third cases in Figures 5(b) and 5(c), the pressure gradient is not parallel, and an inclination is observed (implying the presence of two pressure gradient components) due to the presence of an anisotropic permeability component. In Figure 5(c), one can also observe that at the end of the mold, the flow at the lower edge is distinctly delayed in comparison to the flow at the upper edge due to race-tracking.

Table 1. Comparison of permeability values predicted by proposed methodology for three different cases.

Trial	Lower Limit	Upper Limit	Permeability	Ground Value (m ²)	Predicted Value (m ²)	Relative Error (%)	Number of Iterations	Elapsed Time (sec.)
Case 1. Isotropic preform – regular mold domain								
a.	2.00E-11	2.00E-09	K _{xx}	5.65 x 10 ⁻¹⁰	5.65 x 10 ⁻¹⁰	6.40 x 10 ⁻⁴	37	3924.407
b.	2.00E-11	2.00E-09	K _{xx}	2.00 x 10 ⁻¹⁰	2.00 x 10 ⁻¹⁰	1.63 x 10 ⁻³	34	3750.131
Case 2. Anisotropic preform – mold domain with disturbance								
a.	2.00E-11	2.00E-09	K _{xx}	5.65 x 10 ⁻¹⁰	5.65 x 10 ⁻¹⁰	0	96	12440.06
	2.50E-11	2.50E-09	K _{yy}	6.35 x 10 ⁻¹⁰	6.35 x 10 ⁻¹⁰	0		
	1.00E-12	1.00E-10	K _{xy}	1.97 x 10 ⁻¹¹	1.97 x 10 ⁻¹¹	0		
b.	2.00E-11	2.00E-09	K _{xx}	2.00 x 10 ⁻¹⁰	2.00 x 10 ⁻¹⁰	0	212	29833.51
	2.50E-11	2.50E-09	K _{yy}	2.50 x 10 ⁻¹⁰	2.50 x 10 ⁻¹⁰	0		
	1.00E-12	1.00E-10	K _{xy}	2.23 x 10 ⁻¹¹	2.23 x 10 ⁻¹¹	0		
Case 3. Anisotropic preform with the presence of race-tracking – mold domain with disturbance								
a.	2.00E-11	2.00E-09	K _{xx}	5.65 x 10 ⁻¹⁰	5.65 x 10 ⁻¹⁰	1.77 x 10 ⁻³	173	33931.864
	2.50E-11	2.50E-09	K _{yy}	6.35 x 10 ⁻¹⁰	6.35 x 10 ⁻¹⁰	2.36 x 10 ⁻²		
	1.00E-12	1.00E-10	K _{xy}	1.97 x 10 ⁻¹¹	1.97 x 10 ⁻¹¹	7.61 x 10 ⁻²		
	1.00E-09	1.00E-07	K _{rt}	1.00 x 10 ⁻⁸	1.00 x 10 ⁻⁸	3.00 x 10 ⁻²		
b.	2.00E-11	2.00E-09	K _{xx}	2.00 x 10 ⁻¹⁰	1.99 x 10 ⁻¹⁰	3.82 x 10 ⁻¹	800	95381.674
	2.50E-11	2.50E-09	K _{yy}	2.50 x 10 ⁻¹⁰	2.60 x 10 ⁻¹⁰	3.96 x 10 ⁰		
	1.00E-12	1.00E-10	K _{xy}	2.23 x 10 ⁻¹¹	2.22 x 10 ⁻¹¹	4.20 x 10 ⁻¹		
	1.00E-09	1.00E-07	K _{rt}	1.00 x 10 ⁻⁸	1.02 x 10 ⁻⁸	2.06 x 10 ⁰		

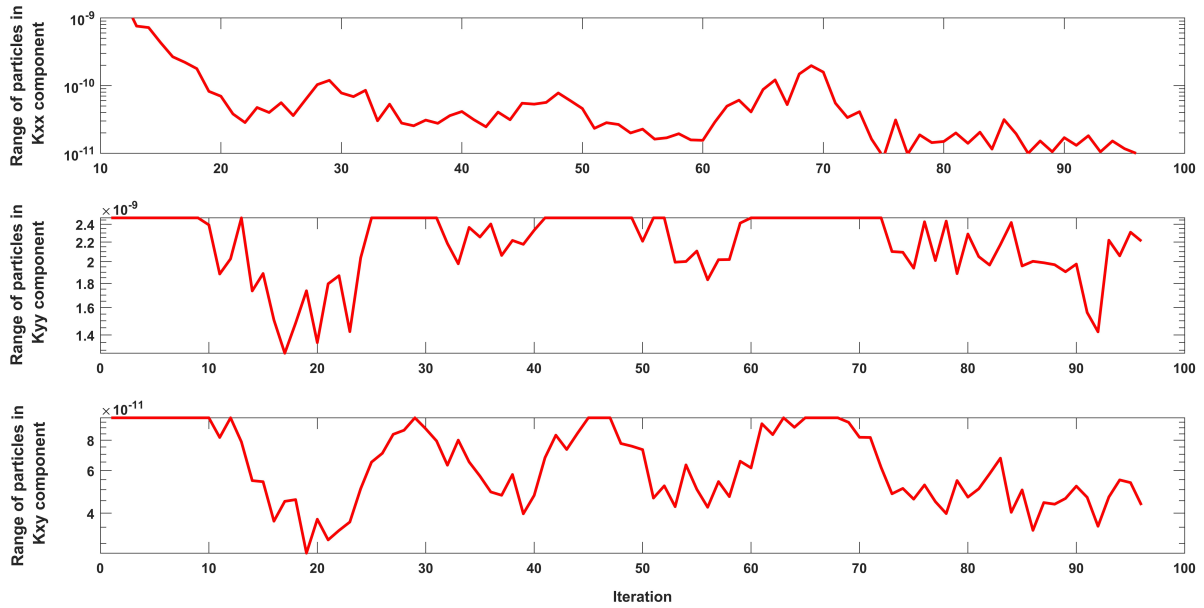


Figure 5. Evolution of the population of particles in each variable direction for Case 2 (a) of Table 1.

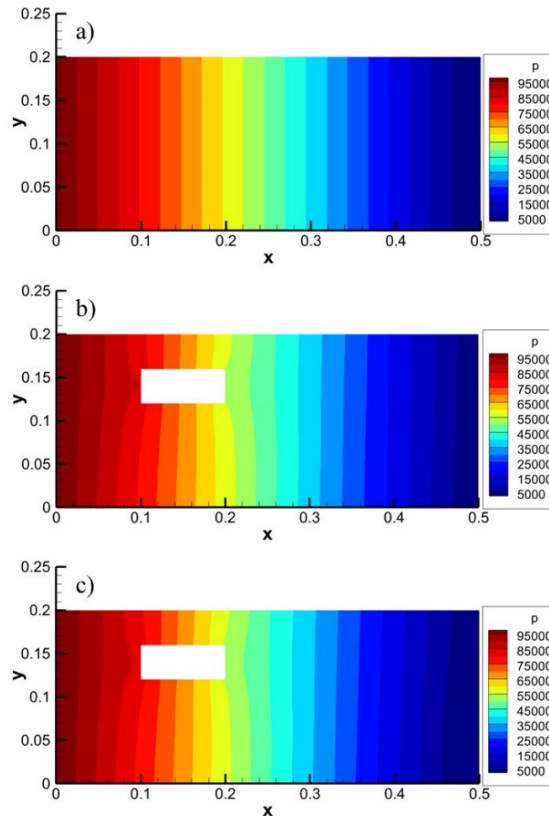


Figure 6. Pressure distribution for (a) isotropic preform – regular mold, (b) anisotropic preform – mold with disturbance, and (c) anisotropic preform with presence of race-tracking – mold with disturbance.

The discretized geometry used for the virtual experiment for case (iii) has 1044 nodes, and as previously mentioned, these nodes correspond to the position of sensors used in the actual experiment to record experimental flow arrival time. To use these many sensors in an experiment is not efficient and requires a substantial amount of effort, which is contrary to the objective of the present study. Therefore, additional analyses have been made to observe the effect of the number of nodes/sensors on the prediction behavior of the proposed methodology. The aim of the study is to find the minimum number of nodes/sensors sufficient to predict permeability values with minimum error in less time. Hence, time to get predicted values along with an average of errors associated with each permeability component is plotted against different numbers of nodes/sensors for two different sets of permeabilities (Figure 7). The observed general trend for both cases is quite similar, i.e., there

is a trade-off between total elapsed time and average error. After observing the elapsed time and average error for each case, it can be concluded that ten nodes/sensors give the best combination of elapsed time and average error, and it can be considered an optimum number of sensors required to predict permeability components in a time-efficient manner.

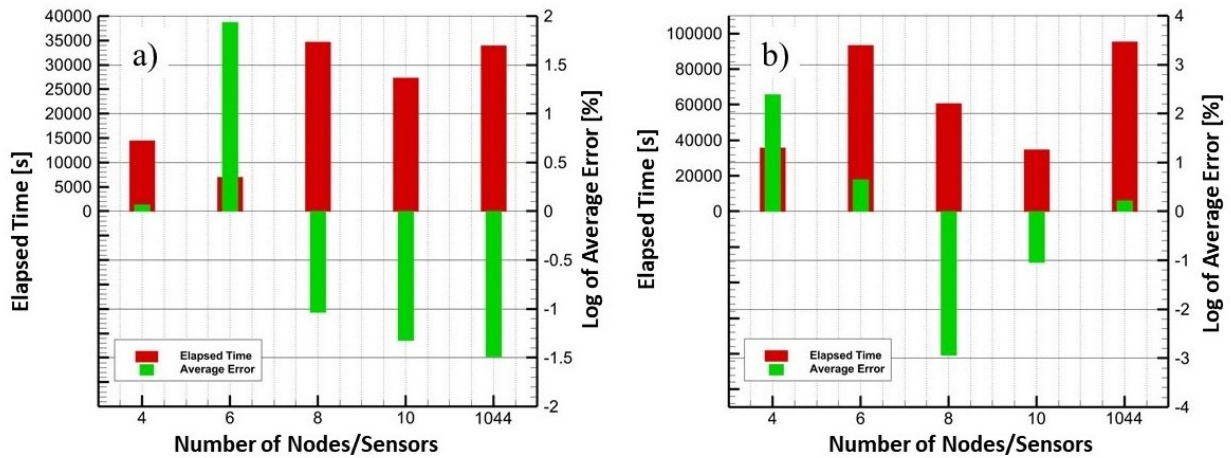


Figure 7. Effect of number of nodes/sensors on the prediction behavior of proposed methodology.

4. Conclusion

A methodology based on disturbing a unidirectional resin flow has been proposed to predict all three components of in-plane permeability tensor from a single rectilinear flow experiment. The method depends on recording the resin flow arrival times during the experiment and minimizing the error between experimental resin flow arrival time and numerical resin flow arrival time obtained via RTM simulation of a similar mold domain in LIMS. The residual sum of squares (RSS) is used to define the error between the experimental and numerical resin arrival time, and the particle swarm optimization (PSO) algorithm is used to minimize this error. Three different cases were performed, each containing two different sets of permeabilities. The proposed methodology has successfully predicted the permeability with high accuracy for all three cases. An analysis to determine the least number of nodes/sensors sufficient for permeability prediction has been performed to reduce the excessive efforts required in the prediction process. It is found that ten nodes/sensors will be enough to determine the accurate permeability values from a single rectilinear experiment, specifically for the geometry that used in this study.

Acknowledgment

The authors would like to thank Dr. Pavel Simacek and Prof. Suresh G. Advani from the University of Delaware for their advisement on LIMS implementation. This research did not receive any specific grant from funding agencies in the public, commercial, or not-for-profit sectors.

References

- [1] M. Seyednourani, M. Yildiz, and H. S. Sas, "A two-stage optimization methodology for gate and vent locations and distribution media layout for liquid composite molding process," *Compos. Part A Appl. Sci. Manuf.*, vol. 149, no. June, p. 106522, 2021, doi: 10.1016/j.compositesa.2021.106522.
- [2] S. Jiang, C. Zhang, and B. Wang, "Optimum arrangement of gate and vent locations for RTM process design using a mesh distance-based approach," *Compos. Part A Appl. Sci. Manuf.*, vol. 33, no. 4, pp. 471–481, Apr. 2002, doi: 10.1016/S1359-835X(01)00146-4.
- [3] H. S. Sas and M. Erdal, "Modeling of particle–resin suspension impregnation in compression resin transfer molding of particle-filled, continuous fiber reinforced composites," *Heat Mass Transf.*, vol. 50, no. 3, pp. 397–414, Mar. 2014, doi: 10.1007/s00231-013-1275-z.
- [4] T. S. Lundström, B. R. Gebart, and E. Sandlund, "In-plane permeability measurements on fiber reinforcements by the multi-cavity parallel flow technique," *Polym. Compos.*, vol. 20, no. 1, pp. 146–154, Feb. 1999, doi: 10.1002/PC.10342.
- [5] C. Di Fratta, G. Koutsoukis, F. Klunker, F. Trochu, and P. Ermanni, "Characterization of anisotropic permeability from flow front angle measurements," *Polym. Compos.*, vol. 37, no. 7, pp. 2037–2052, Jul. 2016, doi: 10.1002/PC.23382.
- [6] K. K. Han, C. W. Lee, and B. P. Rice, "Measurements of the permeability of fiber preforms and

- applications," *Composites Science and Technology*, vol. 60, no. 12–13, pp. 2435–2441, 2000, doi: 10.1016/S0266-3538(00)00037-3.
- [7] P. Ferland, D. Guittard, and F. Trochu, "Concurrent methods for permeability measurement in resin transfer molding," *Polym. Compos.*, vol. 17, no. 1, pp. 149–158, Feb. 1996, doi: 10.1002/PC.10600.
- [8] J. R. Weitzenböck, R. A. Sheno, and P. A. Wilson, "A unified approach to determine principal permeability of fibrous porous media," *Polym. Compos.*, vol. 23, no. 6, pp. 1132–1150, Dec. 2002, doi: 10.1002/PC.10507.
- [9] E. Fauster *et al.*, "Image processing and data evaluation algorithms for reproducible optical in-plane permeability characterization by radial flow experiments," <https://doi.org/10.1177/0021998318780209>, vol. 53, no. 1, pp. 45–63, Jun. 2018, doi: 10.1177/0021998318780209.
- [10] B. R. Gebart and P. Lidström, "Measurement of in-plane permeability of anisotropic fiber reinforcements," *Polym. Compos.*, vol. 17, no. 1, pp. 43–51, 1996, doi: 10.1002/PC.10589.
- [11] T. S. Lundström, R. Stenberg, R. Bergström, H. Partanen, and P. A. Birkeland, "In-plane permeability measurements: a nordic round-robin study," *Compos. Part A Appl. Sci. Manuf.*, vol. 31, no. 1, pp. 29–43, Jan. 2000, doi: 10.1016/S1359-835X(99)00058-5.
- [12] R. S. Parnas and A. J. Salem, "A comparison of the unidirectional and radial in-plane flow of fluids through woven composite reinforcements," *Polym. Compos.*, vol. 14, no. 5, pp. 383–394, Oct. 1993, doi: 10.1002/PC.750140504.
- [13] N. Vernet *et al.*, "Experimental determination of the permeability of engineering textiles: Benchmark II," *Compos. Part A Appl. Sci. Manuf.*, vol. 61, pp. 172–184, 2014, doi: 10.1016/j.compositesa.2014.02.010.
- [14] W. R. Hwang and S. G. Advani, "Numerical simulations of Stokes–Brinkman equations for permeability prediction of dual scale fibrous porous media," *Phys. Fluids*, vol. 22, no. 11, p. 113101, Nov. 2010, doi: 10.1063/1.3484273.
- [15] K. Okonkwo, P. Simacek, S. G. Advani, and R. S. Parnas, "Characterization of 3D fiber preform permeability tensor in radial flow using an inverse algorithm based on sensors and simulation," *Compos. Part A Appl. Sci. Manuf.*, vol. 42, no. 10, pp. 1283–1292, 2011, doi: 10.1016/j.compositesa.2011.05.010.
- [16] M. Yun, H. Sas, P. Simacek, and S. G. Advani, "Characterization of 3D fabric permeability with skew terms," *Compos. Part A Appl. Sci. Manuf.*, vol. 97, pp. 51–59, 2017, doi: 10.1016/j.compositesa.2016.12.030.
- [17] A. Gokce, M. Chohra, S. G. Advani, and S. M. Walsh, "Permeability estimation algorithm to simultaneously characterize the distribution media and the fabric preform in vacuum assisted resin transfer molding process," *Compos. Sci. Technol.*, vol. 65, no. 14, pp. 2129–2139, Nov. 2005, doi: 10.1016/j.compscitech.2005.05.012.
- [18] J. Lugo, P. Simacek, and S. G. Advani, "Analytic method to estimate multiple equivalent permeability components from a single rectilinear experiment in liquid composite molding processes," *Composites Part A: Applied Science and Manufacturing*, vol. 67, pp. 157–170, 2014, doi: 10.1016/j.compositesa.2014.08.031.
- [19] P. Šimáček and S. G. Advani, "Desirable features in mold filling simulations for liquid composite molding processes," *Polym. Compos.*, vol. 25, no. 4, pp. 355–367, 2004, doi: 10.1002/pc.20029.
- [20] S. Bickerton, H. C. Stadtfeld, K. V Steiner, and S. G. Advani, "Design and application of actively controlled injection schemes for resin-transfer molding," *Compos. Sci. Technol.*, vol. 61, no. 11, pp. 1625–1637, Aug. 2001, doi: 10.1016/S0266-3538(01)00064-1.
- [21] E. . Sozer, S. Bickerton, and S. . Advani, "On-line strategic control of liquid composite mould filling process," *Compos. Part A Appl. Sci. Manuf.*, vol. 31, no. 12, pp. 1383–1394, Dec. 2000, doi: 10.1016/S1359-835X(00)00060-9.
- [22] R. Eberhart and James Kennedy, "A New Optimizer Using Particle Swarm Theory," *Int. Symp. Micro Mach. Hum. Sci.*, pp. 39–43, 1999, [Online]. Available: [https://bytebucket.org/12er/pso/raw/b448ff0db375c1ac0c55855e9f19aced08b44ca6/doc/literature/Variants/topology/A new Optimizer using Particle Swarm Theory.pdf](https://bytebucket.org/12er/pso/raw/b448ff0db375c1ac0c55855e9f19aced08b44ca6/doc/literature/Variants/topology/A%20new%20Optimizer%20using%20Particle%20Swarm%20Theory.pdf).
- [23] W.-B. Young and C.-L. Lai, "Analysis of the edge effect in resin transfer molding," *Compos. Part A Appl. Sci. Manuf.*, vol. 28, no. 9–10, pp. 817–822, Jan. 1997, doi: 10.1016/S1359-835X(97)00034-1.
- [24] S. Bickerton, S. G. Advani, R. V. Mohan, and D. R. Shires, "Experimental analysis and numerical modeling of flow channel effects in resin transfer molding," *Polym. Compos.*, vol. 21, no. 1, pp. 134–153, Feb. 2000, doi: 10.1002/pc.10172.